WATER RESOURCES RESEARCH, VOL. 29, NO. 4, PAGES 1287–1295, APRIL 1993

Southern Oscillation Effects on Daily Precipitation in the Southwestern United States

D. A. WOOLHISER AND T. O. KEEFER

Agricultural Research Service, U.S. Department of Agriculture, Tucson, Arizona

K. T. REDMOND

Western Regional Climate Center, Reno, Nevada

The effect of the Southern Oscillation on daily precipitation in the southwestern United States is examined by using the Southern Oscillation Index (SOI) to perturb parameters of a stochastic daily precipitation model. Daily precipitation is modeled with a Markov chain-mixed exponential model and seasonal variability of model parameters is described by Fourier series. The hypothesized linkage between the SOI and the model parameters is of the form $G_i(N, t) = G_i(t) + b_i S(N, t - \tau_i)$ where $G_i(N, t)$ is the perturbed parameter i for day t of year N, $G_i(t)$ is the annually periodic parameter i for day t, b_i is a coefficient, S is the SOI, and τ_i is a lag in days. Daily precipitation data for 27 stations in California, Nevada, Arizona, and New Mexico were analyzed. Perturbations of the logits of the dry-dry transition probabilities resulted in statistically significant improvements in the log likelihood function for 23 stations and perturbations of the mean daily rainfall resulted in significant increases for 18 stations. The most common lag identified was 90 days, suggesting the possibility of conditional simulations of daily precipitation. Seasonal effects were detected, confirming the results of previous analysis with groups of stations.

INTRODUCTION

The coupled atmosphere-ocean system exemplified by the El Nino-Southern Oscillation (ENSO) and its impact on weather and weather-related phenomena has recently been the subject of much scientific interest. Several studies have shown statistical relationships between ENSO and weather patterns and precipitation [*Caviedes*, 1975, 1984; *Yarnal and Diaz*, 1986; *Andrade and Sellers*, 1988; *Kiladis and Diaz*, 1989; *Ropelewski and Halpert*, 1986, 1987, 1989, 1990; *Schonher and Nicholson*, 1989; *Redmond and Koch*, 1991]. Others have investigated the relationship between ENSO and precipitation dependent phenomena such as tree growth [*Lough and Fritts*, 1985], fire scars [*Swetnam and Betancourt*, 1990], and floods [*Webb and Betancourt*, 1990].

Stochastic models of daily precipitation with annually periodic parameters usually do not preserve the variances of monthly and annual precipitation [*Buishand*, 1977; *Zucchini and Adamson*, 1984; *Woolhiser et al.*, 1988]. This characteristic underestimation may be due to real long-term trends in precipitation, changes in data collection techniques or in rain gage exposure, model inadequacies, and/or the existence of large-scale atmospheric circulation patterns that do not exhibit annual periodicities. The Southern Oscillation (SO) is an example of such a pattern and is defined as "... a coherent variation of barometric pressures at interannual intervals that is related to weather phenomena on a global scale, particularly in the tropics and subtropics" [*Enfield*, 1989, p. 161]. The SO is quantitatively described by the SOI, the time series of the anomalies of atmospheric pressure differences between Papeete, Tahiti, and Darwin, Australia. The SOI is well correlated with equatorial sea surface temperatures in the Eastern Pacific [*Rasmussen and Wallace*, 1983].

Techniques to identify ENSO effects include (1) regressions between annual or seasonal precipitation for groups of stations and SOI and (2) testing for differences in the mean precipitation between years classified as ENSO or non-ENSO. *Woolhiser* [1992] proposed a new technique to identify ENSO effects on precipitation. The essence of this method is to use the SOI as a function to perturb the parameters of a stochastic daily precipitation model. In this model the occurrence of wet days is described by a first-order Markov chain, the distribution of precipitation depth, given a wet day, is described by a mixed exponential distribution, and Fourier series are used to describe seasonal variations in the five parameters required. In a preliminary study *Woolhiser* [1992] detected SOI effects on the dry-dry transition probabilities of the first-order Markov chain for four Arizona stations and two Idaho stations but did not detect an effect for two Idaho stations and three Oregon stations. However, he did find significant effects on the mean daily precipitation (given a wet day) for all stations. The effects in the Southwest were opposite of those in the Northwest with negative SOI (El Nino) leading to more frequent precipitation and increased depths of daily precipitation in Arizona. The most frequent lag was about 90 days with the SOI leading precipitation. *Horel and Wallace* [1981] have pointed out the existence of a lagged connection between the tropical Pacific and higher latitudes in a model atmosphere.

The objective of the research reported here was to use the procedure suggested by *Woolhiser* [1992] to analyze SOI impacts on precipitation in the southwestern United States including stations in California, Nevada, Arizona, and New Mexico.

Paper number 92WR02536.
0043-1397/93/92WR-02536$05.00

MODEL OF DAILY PRECIPITATION

Occurrence

We will assume that the daily occurrence of precipitation can be described by a first-order Markov chain. Let

$$X(t) = 0 \quad \text{if day } t \text{ is dry} \quad t = t_1, \cdots t_T \tag{1a}$$

$$X(t) = 1$$

if day t has rain equal to or greater than a threshold, d (1b)

Let the daily transition probabilities be written as

$$P_{ij}(t) = P[X(t) = j | X(t-1) = i] \qquad i, j = 0, 1 \tag{2}$$

Because $P_{i0}(t) + P_{i1}(t) = 1$, only two parameters are required for each day. $P_{00}(t)$ and $P_{10}(t)$ were used in this study.

Amount

Let $Y(t)$ be the amount of precipitation on day t when $X(t) = 1$. We assume that $Y(t)$ is serially independent and is also independent of $X(t-1)$. Let the random variable $U(t) = Y(t) - d$ be distributed as a mixed exponential (ME)

$$f_t(u) = \alpha(t)/\beta(t) \exp[-u/\beta(t)] + [1 - \alpha(t)]/\delta(t) \exp[-u/\delta(t)] \tag{3}$$

where $0 < u < \infty$, d is a threshold (normally 0.01 inch or 0.25 mm), $0 < \alpha(t) < 1$, and $0 < \beta(t) < \delta(t)$. The mean $\mu(t)$ is given by

$$\mu(t) = \alpha(t)\beta(t) + [1 - \alpha(t)]\delta(t) \tag{4a}$$

and the variance is

$$\sigma^2(t) = 2\alpha(t)\beta(t)^2 + 2[1 - \alpha(t)]\delta(t)^2 - \{\alpha(t)\beta(t) + [1 - \alpha(t)]\delta(t)\}^2 \tag{4b}$$

Seasonal Variability

To account for the seasonal variability of the parameters of the Markov chain-mixed exponential model, the parameters $p_{00}(t)$, $p_{10}(t)$, $\alpha(t)$, $\beta(t)$, and $\mu(t)$ are written in the polar form of a finite Fourier series:

$$G_i(t) = G_{i0} + \sum_{k=1}^{m_i} [C_{ik} \sin(2\pi tk/365 + \phi_{ik})] \tag{5}$$

where $i = 1, 2, \cdots, 5$, $G_i(t)$ is the value of the ith parameter on day t, m_i is the maximum number of harmonics, G_{i0} is the mean, C_{ik} is the amplitude of the kth harmonic, and Φ_{ik} is the phase angle of the kth harmonic for the ith parameter.

So that constraints need not be imposed, the logit transform of the transition probabilities are fit with Fourier series as demonstrated by *Stern and Coe* [1984] and *Zucchini and Adamson* [1984]:

$$g_{ij}(t) = \log\{p_{ij}(t)/[1 - p_{ij}(t)]\} \qquad -\infty < g_{ij}(t) < +\infty \tag{6}$$

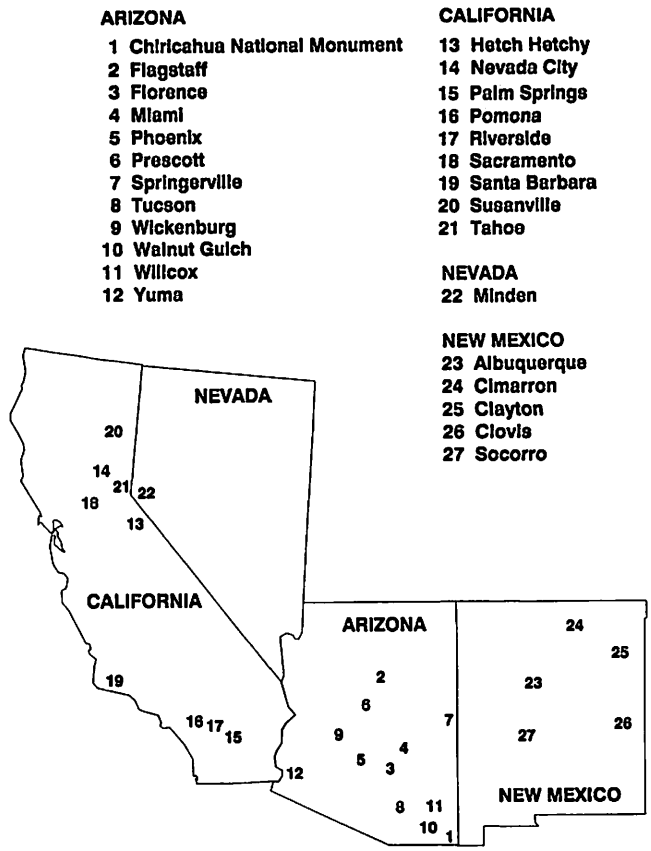

Fig. 1. Location map.

The transition probabilities are obtained by the inverse transform

$$p_{ij}(t) = \exp[g_{ij}(t)]/\{1 + \exp[g_{ij}(t)]\} \tag{7}$$

SOI perturbation linkage. To utilize the SOI as a perturbing factor for the daily precipitation model, we must hypothesize the form of the linkage between the SOI and model parameters. *Woolhiser* [1992] used the following linear form:

$$G_i(N, t) = G_i(t) + b_i S(N, t - \tau_i) \tag{8}$$

where $G_i(N, t)$ is the perturbed parameter i on day t of year N, and the coefficient b_i and the lag in days τ_i are parameters to be estimated from the data and $S(t)$ is the SOI on day t. The logits of both Markov chain transition probabilities, $g_{00}(t)$ and $g_{10}(t)$, and the mean of the ME, $\mu(t)$, were assumed to be affected by the SOI. All perturbations in the mean $\mu(t)$ were transferred to the parameter $\delta(t)$, which can be interpreted as the mean of the largest exponential distribution in the mixture. From (4a) and (4b) we note that an increase in $\mu(t)$ due to perturbation by the SOI will also lead to an increase in the variance $\sigma^2(t)$.

Identification of parameters. The parameters were identified in a two-stage procedure. First, the Fourier coefficients that describe the purely periodic seasonal variation of the parameters were estimated for each station. Then the SOI linkage parameters were estimated independently. The Fourier coefficients for the logits, $g_{00}(t)$ and $g_{10}(t)$, were estimated by maximum likelihood techniques as described in the

TABLE 1. Statistics of Precipitation Stations Analyzed

Station	Elevation Above Sea Level, m	Length of Record, years	Annual Precipitation		Annual No. of Wet Days	
			Mean, mm	Standard Deviation, mm	Mean, days	Standard Deviation, days
			Arizona			
Chiricahua National Monument	1615	40	485.14	130.56	70.63	12.37
Flagstaff	2105	32	526.29	140.21	77.72	13.76
Florence	455	55	248.16	84.58	38.55	9.35
Miami	1095	55	473.71	149.86	58.55	11.81
Phoenix	335	33	76.78	67.56	34.39	8.45
Prescott	1630	80	492.76	133.86	65.21	12.87
Springerville	2120	77	303.53	83.56	61.96	15.93
Tucson	735	94	282.70	88.90	48.93	10.37
Wickenburg	630	38	272.29	97.03	36.95	7.51
Walnut Gulch	1272	33	305.31	82.55	53.61	13.07
Willcox	1280	30	322.33	97.79	59.70	12.74
Yuma	35	31	73.66	52.07	15.81	7.51
			California			
Hetch Hetchy	1180	58	863.85	248.41	70.33	13.58
Nevada City	790	55	1,398.27	376.94	81.76	13.21
Palm Springs	130	62	143.51	86.87	17.71	7.13
Pomona	260	55	436.63	181.36	36.85	9.69
Riverside	275	54	259.59	112.52	35.20	8.86
Sacramento	10	55	469.65	155.70	58.80	12.10
Santa Barbara	35	50	430.28	152.15	34.76	8.28
Susanville	1265	58	362.46	124.21	62.05	12.88
Tahoe	1900	55	806.96	271.02	78.82	13.88
			Nevada			
Minden	1440	44	214.12	64.77	41.50	11.30
			New Mexico			
Albuquerque	1620	55	215.14	63.25	60.02	12.48
Cimarron	1960	55	384.81	96.52	65.13	14.48
Clayton	1525	55	377.70	136.40	65.04	14.47
Clovis	1305	55	440.18	161.80	53.11	11.68
Socorro	1410	52	224.03	67.56	44.81	10.83

appendix, and the coefficients for the ME parameters, α, $\beta(t)$, and $\mu(t)$ were estimated by numerical maximum likelihood methods described by *Woolhiser and Roldan* [1986]. The parameter α was considered to be time invariant as they recommended.

By incorporating the SOI perturbations as given by (8) the log likelihood function can be written as a function of the parameters b_i and τ_i. It can be shown that the log likelihood functions for the dry-dry transitions are independent of the log likelihood functions for the wet-dry transitions [*Woolhiser and Pegram*, 1979]. Thus the parameters b_{00}, b_{10}, τ_{00}, τ_{10}, b_μ, and τ_μ can be estimated by a series of three bivariate optimizations.

Analysis of Data

Daily precipitation data were obtained for 27 stations in California, Nevada, Arizona, and New Mexico. They were chosen to provide a sharp contrast between the Mediterranean climate of southern California and the predominantly summer precipitation regime of eastern New Mexico. They also sampled a wide range in elevation and mean annual precipitation. Station locations are shown in Figure 1, and a list of the stations, station elevations, and some statistical characteristics of the precipitation regimes are shown in Table 1.

A monthly SOI series for the period January 1933 through November 1989 was obtained from the National Oceanic and Atmospheric Administration (NOAA) Climate Analysis Center. This SOI is a standardized series obtained from the

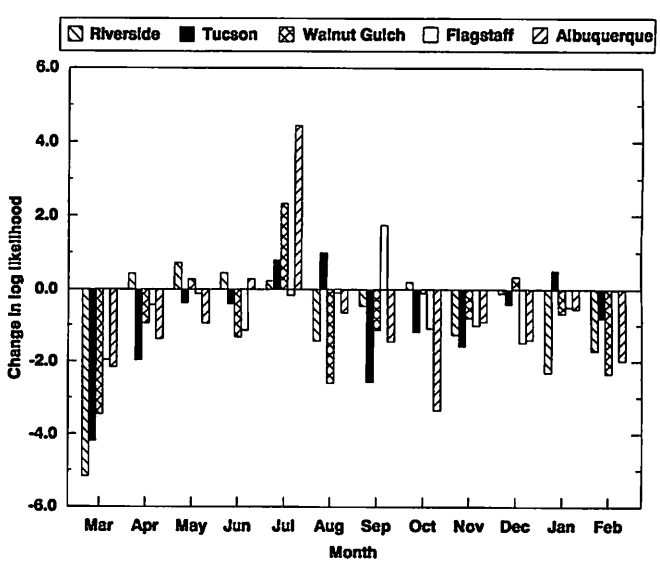

Fig. 2. Change in log likelihood function due to setting b_{00} to 0 for each month.

TABLE 2. Effect of SOI Perturbations of the Logit of the Markov Chain Dry-Dry Transition Probability

Station	Unperturbed Log Likelihood	All Year Perturbed: Increase Over Unperturbed Log Likelihood	All Year Perturbed: b_{00}	All Year Perturbed: τ_{00}, days	One Season Unperturbed: Season	One Season Unperturbed: Increase Over Perturbed Log Likelihood	One Season Unperturbed: b_{00}	One Season Unperturbed: τ_{00}, days
			Arizona					
Chiricahua National Monument	−5,877.764	9.984	+0.12	30	Sept.	1.720	+0.14	30
Flagstaff	−5,149.836	6.350	+0.11	150	Sept.	1.988	+0.13	150
Florence	−6,028.583	6.900	+0.10	90	July	1.440	+0.12	30
Miami	−7,584.766	7.641	+0.10	90	July to August	3.632	+0.13	90
Phoenix	−3,306.461	5.453	+0.13	0	July	2.163	+0.16	0
Prescott	−8,036.973	9.148	+0.11	0	July	1.193	+0.12	0
Springerville	−8,110.575	24.325	+0.17	90	July	4.295	+0.19	90
Tucson	−6,861.882	11.178	+0.12	90	July to August	2.459	+0.15	90
Walnut Gulch	−4,140.268	10.500	+0.15	90	July	2.650	+0.18	90
Wickenburg	−3,923.870	7.667	+0.14	90	May	0.776	+0.15	90
Willcox	−4,142.630	9.882	+0.14	90	May to June	0.843	+0.15	90
Yuma	−1,717.268	6.723	+0.19	90	April to August	2.544	+0.20	90
			California					
Hetch Hetchy	−7,641.140	6.397	+0.09	0	Nov.	1.680	+0.11	0
Nevada City	−7,848.420	1.517*	+0.05	240	Sept. to Oct.	1.987	+0.07	240
Palm Springs	−3,269.061	17.502	+0.15	120	May to July	4.184	+0.20	120
Pomona	−5,153.902	3.430	+0.08	150	May to July	3.582	+0.12	150
Riverside	−4,985.657	10.520	+0.14	120	April to July	1.730	+0.16	150
Sacramento	−6,763.485	3.470	+0.07	150	April	0.922	+0.08	150
Santa Barbara	−4,024.504	3.867	+0.11	330	April to May	1.258	+0.13	330
Susanville	−7,777.478	1.828*	+0.05	120	Oct.	0.970	+0.06	120
Tahoe	−8,472.088	1.386*	+0.04	0	Oct. to Dec.	2.586	+0.08	0
			Nevada					
Minden	−5,107.768	1.475*	+0.05	0	Oct. to Jan.	2.226	+0.10	0
			New Mexico					
Albuquerque	−8,245.569	10.133	+0.10	120	July	5.572	+0.14	120
Cimarron	−8,305.203	8.605	+0.09	60	June	1.384	+0.11	60
Clayton	−8,547.185	5.930	+0.08	90	June to Sept.	3.931	+0.13	30
Clovis	−7,597.107	6.582	+0.09	90	July to Sept.	2.955	+0.13	90
Socorro	−6,339.205	5.119	−0.09	360	Aug. to Sept.	1.034	−0.11	360

SOI, Southern Oscillation Index.
*No significant increase in log likelihood function.

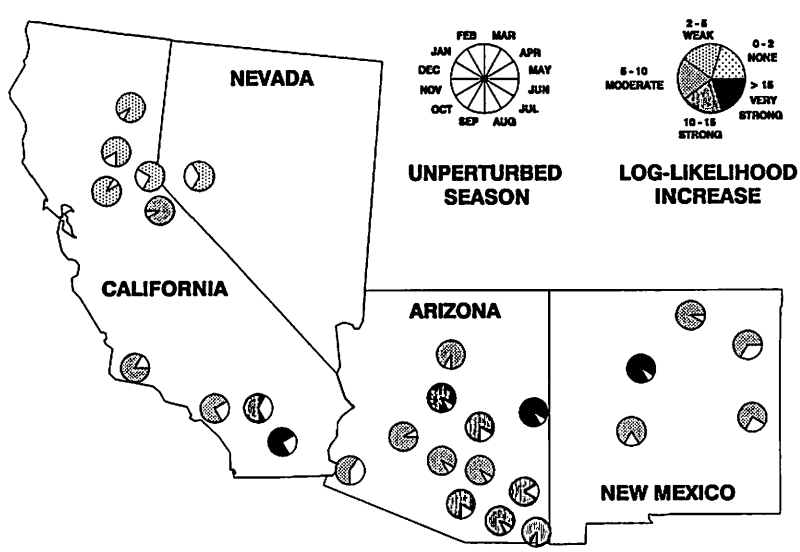

Fig. 3. Seasonal effects: Markov chain.

TABLE 3. Effect of SOI Perturbations of the Mean of the Mixed Exponential Distribution

Station	Unperturbed Log Likelihood	All Year Perturbed: Increase Over Unperturbed Log Likelihood	All Year Perturbed: b_μ	All Year Perturbed: τ_μ, days	One Season Unperturbed: Season	One Season Unperturbed: Increase Over Perturbed Log Likelihood	One Season Unperturbed: b_μ	One Season Unperturbed: τ_μ, days
			Arizona					
Chiricahua National Monument	1,285.297	1.659*	−0.010	90	July	3.243	−0.016	240
Flagstaff	1,106.610	3.636	−0.017	90	Apr.	1.714	−0.020	90
Florence	1,008.434	2.896	−0.016	90	Nov.	0.925	−0.019	90
Miami	853.498	2.453	−0.014	90	July	3.100	−0.020	90
Phoenix	872.973	3.207	−0.017	90	Jan.	1.029	−0.020	90
Prescott	1,616.810	3.772	−0.017	60	May	0.981	−0.019	60
Springerville	3,087.966	1.172*	+0.001	30	July	8.040	+0.009	150
Tucson	1,720.264	4.422	−0.016	60	March to July	1.699	−0.020	60
Walnut Gulch	1,092.488	4.238	−0.016	90	April to July	2.723	−0.020	0
Wickenburg	462.805	2.202	−0.018	60	Jan.	0.763	−0.020	60
Wilcox	1,266.781	1.749*	−0.010	90	June to July	3.980	−0.017	240
Yuma	451.237	0.643*	−0.009	60	Jan. to Feb.	2.086	−0.020	120
			California					
Hetch Hetchy	−549.253	0.708*	+0.009	180	April	0.988	+0.016	180
Nevada City	−2,063.768	3.029	−0.020	240	May	0.800	−0.024	240
Palm Springs	334.003	1.531*	−0.019	0	Jan. to Feb.	2.396	−0.024	0
Pomona	−89.719	5.639	−0.020	120	Dec. to Jan.	0.558	−0.020	120
Riverside	710.478	4.426	−0.016	60	March	0.477	−0.017	60
Sacramento	1,134.103	10.116	−0.020	240	May to July	1.937	−0.020	240
Santa Barbara	−31.530	3.805	−0.020	90	May to June	0.777	−0.020	90
Susanville	2,142.940	5.735	+0.013	270	Nov.	1.062	+0.014	270
Tahoe	403.398	3.197	+0.013	270	May	1.018	+0.018	270
			Nevada					
Minden	1,288.167	0.769*	+0.005	30	April	1.306	+0.009	180
			Mew Mexico					
Albuquerque	3,876.325	2.668	−0.006	240	Nov.	0.813	−0.007	240
Cimarron	2,005.777	1.574*	+0.008	330	March to April	1.141	+0.009	300
Clayton	2,552.633	3.939	−0.009	60	Jan.	0.953	−0.011	60
Clovis	746.483	1.146*	+0.008	30	Aug. to Oct.	0.840	+0.011	30
Socorro	1,789.224	2.707	−0.010	180	Feb.	0.994	−0.012	180

SOI, Southern Oscillation Index.
*No significant increase in log likelihood function.

standardized monthly sea level pressure at Papeete, Tahiti, minus the standardized monthly sea level pressure at Darwin, Australia. Because only monthly values were available, $S(N, t)$ was represented as a step function.

Results of perturbing the periodic logit function $g_{00}(t)$ are shown in Table 2, columns 3–5. Only lags of multiples of 30 days were examined in the algorithm to search for the maximum likelihood function of b_i and τ_i. The Akaike information criterion (AIC) [*Akaike*, 1974] was used to determine if the SOI perturbations led to significant increases in the log likelihood functions. The increase in log likelihood due to SOI perturbations led to a minimum AIC for 23 of the 27 stations. The four stations not showing an increase are located in the same geographic area near the Sierra Nevada mountains. In all but one case (Socorro, New Mexico) the optimum coefficient b_{00} ranges from +0.08 to +0.19, but is remarkably consistent from southern California to eastern New Mexico in spite of differences in annual precipitation, elevation, and seasonal patterns. The sign of the coefficient indicates that a negative SOI leads to an increase in the number of wet days. The optimum lag ranges from 0 to 360 days with 90 days being the most frequent value. There is a tendency for longer lags for the California stations. At each location where a significant increase in the log likelihood function was detected, several different lag values produce significant, if not optimal, increases. A 90-day lag resulted in significant increases at 19 of the 23 locations. Perturbing b_{10} did not result in significant increases in the log likelihood function. Thus for negative SOI, a dry day is more likely to be followed by a wet day, but there is no increase in the probability of a wet day following a wet day. Also, the square of the SOI was used as the perturbing factor for five stations, but this resulted in lower maximum likelihood functions for most cases.

Results of perturbing the seasonally varying mean of the mixed exponential distribution, $\mu(t)$, are shown in Table 3 (third, fourth, and fifth columns from the left). Generally, for the 18 locations having a significant increase in the log likelihood function, the coefficients b_μ are negative, which means that with a negative SOI (El Nino condition) the mean and the variance of daily precipitation increases. Two locations, both in the Sierra Nevadas, have positive coefficients indicating decreased daily mean precipitation, a condition found previously at northwestern United States sites [*Wool-*

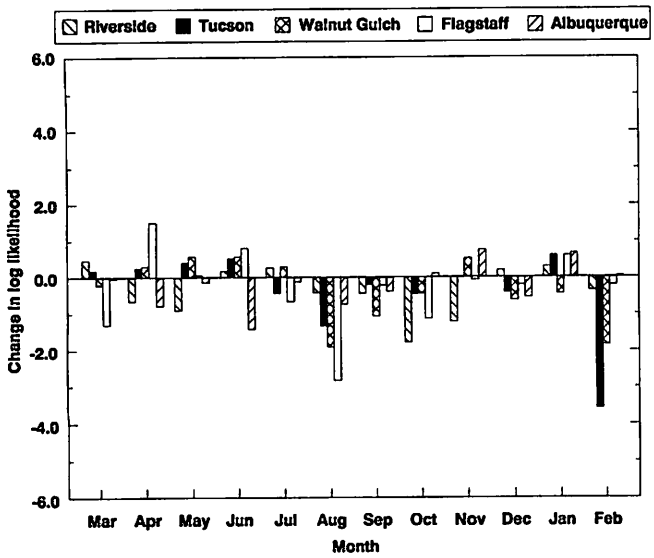

Fig. 4. Change in log likelihood function due to setting b_μ to 0 for each month.

hiser, 1992]. The coefficients decrease from west to east. In California and New Mexico the lag τ_μ has considerable range. The optimum lag in Arizona is 60–90 days.

Seasonal Effects

Several investigators have concluded that the SOI effects on precipitation predominate in certain seasons [*Yarnal and Diaz*, 1986; *Andrade and Sellers*, 1988; *Kiladis and Diaz*, 1989; *Redmond and Koch*, 1991]. In parts of the desert Southwest there are two precipitation maxima, one in winter and one in summer. Summer precipitation is primarily associated with the northward transport of moist tropical air from both the Gulf of Mexico and the subtropical waters off Baja California and is highly convective in nature. Winter precipitation is associated with synoptic scale disturbances and frontal passages. The relative magnitude of these two peaks varies with elevation and longitude, with the wintertime maximum assuming more importance at higher elevations and the summertime maximum being more important in the eastern part of the region. Much of the domain considered here is under the influence of Pacific air masses for at least several months of the year [*Bryson and Hare*, 1974].

Most numerical and observational studies of the extratropical response to tropical sea surface temperature anomalies have focused on winter, when the Northern Hemisphere circulation is more vigorous and extends farther southward, offering more opportunities for tropical–midlatitude interaction [*Horel and Wallace*, 1981; *Rasmussen and Wallace*, 1983; *Schonher and Nicholson*, 1989]. *Redmond and Koch* [1991] found much stronger associations in winter than in summer between precipitation and SOI in this part of the west. The relationship between fire evidence and SOI found by *Swetnam and Betancourt* [1990] centered on growing conditions in spring as influenced by previous precipitation. Other work by *Ropelewski and Halpert* [1986, 1989], *Schonher and Nicholson* [1989], and others have dealt only with winter precipitation. *Cayan and Peterson* [1989] show that ENSO years tend to be characterized by split flow in winter, with the polar jet crossing the coast in Alaska, and a subtropical jet from the Pacific crossing the southern United States. In "anti-ENSO" years the main jet crosses the Pacific Northwest.

Based on the above we would anticipate that the inclusion of b_{00} and b_μ as constants for all months in the analysis would tend to weaken the strength of the SOI-MCME connection. To examine this factor we recalculated the log likelihood functions assuming that the coefficients b_{00} and b_μ successively took on 0 values during each of the 12 months of the year. If the SOI did not influence the precipitation regime for a given month (or if the optimum value for a given month is smaller than the optimum yearly value), we would expect an increase in the log likelihood function if the effect is removed by equating the appropriate monthly coefficient to zero. We performed this analysis for all stations. The changes in the log likelihood functions achieved by setting b_{00} to 0 for each month for Riverside, Flagstaff, Tucson, Walnut Gulch, and Albuquerque are shown in

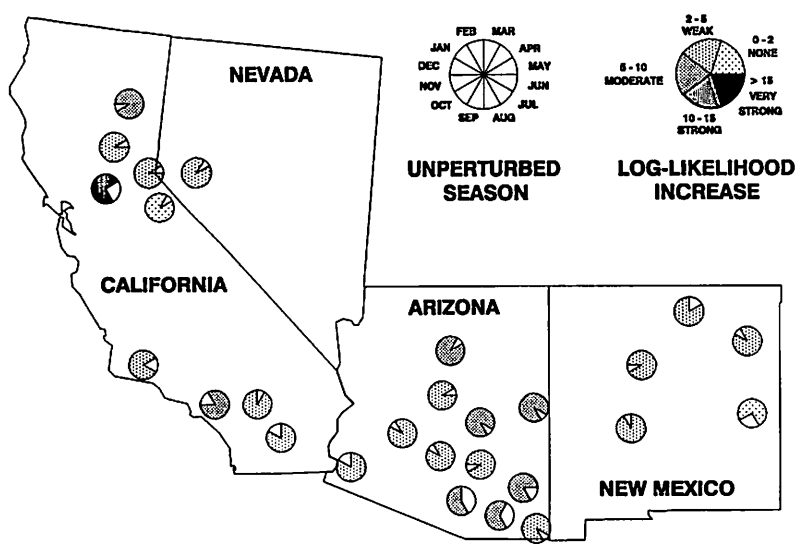

Fig. 5. Seasonal effects: mixed exponential.

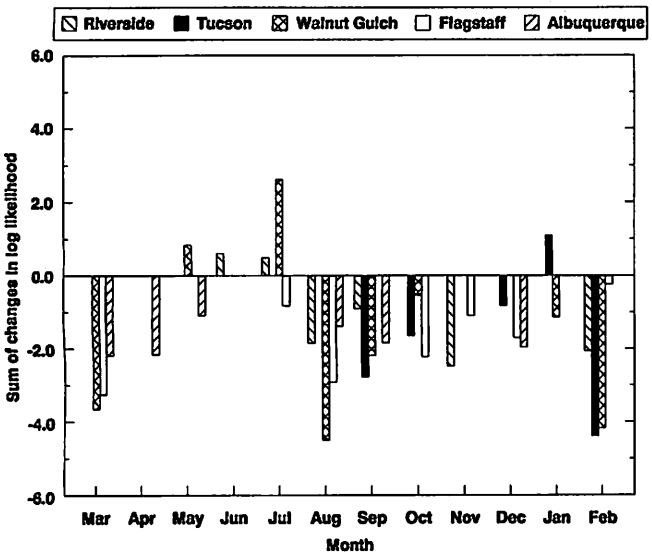

Fig. 6. Sum of the changes in log likelihood functions for Markov chain and mixed exponential when both deviations have the same sign.

Figure 2. A positive deviation indicates that the log likelihood function is increased if the SOI effect is negated (or if the monthly coefficient is reduced), suggesting that the precipitation regime in that month is not sensitive (or is less sensitive) to the atmospheric phenomena in the Pacific Ocean related to the SOI. A large negative deviation indicates a strong relationship.

It is apparent that the SOI perturbation of $g_{00}(t)$ leads to increases in the log likelihood function for most of the year for most of these stations. The effects in February and March are particularly strong. On the other hand, the SOI perturbation is ineffective at Riverside for the period April through July. This coincides with the dry season in southern California. The large positive deviations in July are a striking feature. This pattern may reflect that the Gulf of Mexico is the predominant source of moisture for New Mexico and eastern Arizona in July, while air masses originating in the Pacific occur with increasing frequency in August, September, and October. November exhibits a small, but consistent, negative deviation, while December and January have a preponderance of negative deviations.

Results of this seasonal analysis of the SOI impact on the Markov chain for all stations are shown in Table 2 (four rightmost columns) and are displayed in Figure 3. It is evident that there is a great deal of spatial coherence in the strength of the SOI impact as evidenced by the increase in log likelihood and also the seasonal pattern of the SOI effect. There is no clear evidence for an elevation effect either on the strength of the SOI perturbation or its seasonal pattern.

The deviations of the log likelihood function due to setting the coefficients b_μ to 0 for each month for Riverside, Flagstaff, Tucson, Walnut Gulch, and Albuquerque are shown in Figure 4. Again, the preponderance of deviations are negative, indicating that the mean daily precipitation is related to the SOI. However, the pattern of deviations is somewhat different with negative deviations for all stations in August, September, and October. The three Arizona stations exhibit positive deviations for the period April to June and negative deviations in December and February.

Results of this seasonal analysis of the SOI impact on the mean of the mixed exponential for all stations are shown in Table 3 (four rightmost columns) and are displayed in Figure 5. It is evident that there is some spatial coherence in the strength of the SOI impact as evidenced by the increase in log likelihood but the seasonal pattern of the SOI effect has little spatial coherence. There is no clear evidence for an elevation effect either on the strength of the SOI perturbation or its seasonal pattern.

A comparison of Figures 2 and 4 reveals that for 32 station months the deviations for the Markov chain and mixed exponential are in the same direction (five positive deviations and 27 negative deviations). These summed deviations are plotted in Figure 6. The pattern of deviations suggests that the strongest SOI influence occurs in the period August to October and in February and March. The seasonal patterns exhibited by the deviations suggest that it will be fruitful to investigate methods of identifying parameters of seasonally varying coefficients $b_{00}(t)$ and $b_\mu(t)$.

With the perturbations induced by the SOI with the linkage given by (8), the parameters $p_{00}(t)$ and $\mu(t)$ become random variables. This feature is illustrated in Figure 7

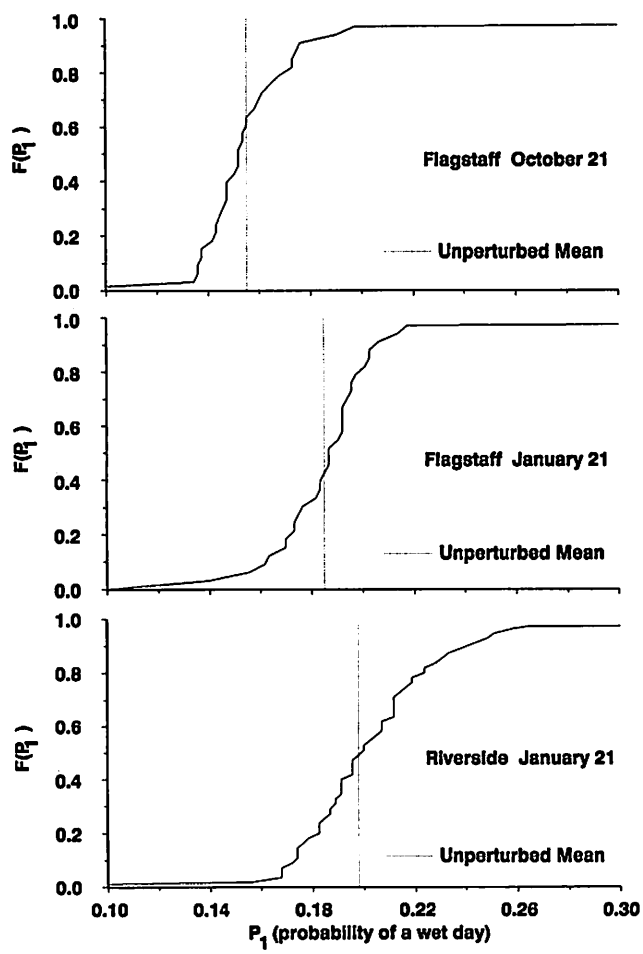

Fig. 7. Empirical distribution function of the probability of a wet day as perturbed by the historical SOI.

where the empirical distribution functions for the probability of precipitation, $P_1 = [1 - p_{00}(t)]/[1 - p_{00}(t) + p_{10}(t)]$ as perturbed by the historical SOI are plotted for selected dates for two stations, Riverside, California and Flagstaff, Arizona. The dates shown coincide with months in which the effect of the SOI is moderate or strong as evidenced by Figure 2. Historical values of the SOI with a 90-day lag were used to perturb G_{00}, and it is clear that these perturbations lead to substantial variation in P_1. Because of the nonlinear nature of the logit transform, the absolute variations in $p_{00}(t)$ are greater when the unperturbed value is close to 0.5 than when it is near 1.

Discussion and Conclusions

The principal objective of this study was to determine if the procedure proposed by *Woolhiser* [1992] could detect effects of the SOI on the daily precipitation regime in the southwestern United States. If the technique resulted in the detection of regionally consistent and physically plausible effects, it could lead to important developments in water management because it offers the possibility of performing precipitation simulations conditioned on past records of SOI. Such simulations, conditioned on the past 90 day records of the SOI, could be carried out for 90 days in the future or possibly longer if the SOI can be predicted [*Chu and Katz*, 1985]. *Wilks* [1989] presented an approach whereby the 30-day precipitation forecasts of the Climate Analysis Center of the NOAA can be used for conditional precipitation simulations. It might be fruitful to investigate a combination of *Wilks* [1989] approach and the techniques outlined in this paper.

On the basis of our analyses we conclude that the technique which uses the SOI to perturb parameters of a stochastic daily precipitation model is effective and has several advantages over previously used methods. It explicitly identifies SOI effects on the frequency of precipitation and on the amounts of precipitation given occurrence. It has a much higher time resolution than previously used methods which typically use seasonal or annual data. This feature allows a more detailed investigation of seasonal effects and may help in relating physical processes to statistically determined SOI—precipitation linkages. Because single stations are used, it is possible to investigate the effect of elevation on these associations. Simulated precipitation sequences with model parameters perturbed by the SOI exhibit greater monthly and annual variances than those simulated with purely periodic parameters. However, it appears that these variances are still underestimated. Additional perturbing factors such as deviations of previous 30-day precipitation from the mean [*Wilks*, 1989] or possible deterministic cycles [*Currie and O'Brien*, 1990] should be investigated.

The effects of the SOI on precipitation are consistent with analyses made by previous investigators but provide higher temporal and spatial resolution. Also, this method does not rely on somewhat arbitrary schemes to classify years as "ENSO" or "NON-ENSO."

Appendix: Parameter Estimation for Markov Chain Model

The approach used to estimate the Fourier coefficients describing the seasonal variation of the parameters of the first-order Markov chain is identical to that used by *Zucchini and Adamson* [1984] and is closely related to the method used by *Stern and Coe* [1984]. Consider M years of observations of precipitation on days t and $t - 1$. The probability mass function of the number of dry days on day t given that day $t - 1$ was dry can be described by the binomial distribution. Therefore the likelihood function for the dry-dry transition probabilities can be written

$$L_{00} = \prod_{t=1}^{365} \binom{N_D(t-1)}{N_{DD}(t)} p_{00}(t)^{N_{DD}(t)} [1 - p_{00}(t)]^{N_D(t-1) - N_{DD}(t)}$$

where $N_D(t - 1)$ is the number of dry days on day $t - 1$ in M years, $N_{DD}(t)$ is the number of dry-dry transitions from day $t - 1$ to day t, and $p_{00}(t)$ is the probability of a dry-dry transition from day $t - 1$ to day t. The log likelihood function can be written as

$$\log L_{00} = \prod_{t=1}^{365} \left[\log \binom{N_D(t-1)}{N_{DD}(t)} + N_{DD}(t) \log p_{00}(t) + \{N_D(t-1) - N_{DD}(t)\} \log \{1 - p_{00}(t)\} \right]$$

Now $p_{00}(t)$ is given by the inverse logit transform, (7), and the logit $G_{00}(t)$ is expressed as a Fourier series with parameters, a_i, $i = 1, 2, \cdots, m_{a_i}$, where m_{a_i} is an odd number.

$$G_{00}(t) = \sum_{i=1}^{m_{a_i}} a_i \phi_i(t)$$

where

$$\phi_i(t) = \cos (i - 1)(2\pi t/365) \qquad i = 1, 3, 5, \cdots$$

$$\phi_i(t) = \sin (2i\pi t/365) \qquad i = 2, 4, \cdots$$

To maximize the log likelihood, we must have

$$\frac{\partial \log L_{00}}{\partial a_i} = 0 \qquad i = 1, 2, \cdots m_{a_i}$$

It can be readily shown that these equations are given by

$$\sum_{t=1}^{365} [N_{DD}(t) - N_D(t-1)] \left\{ \frac{\exp [G_{00}(t)]}{1 + \exp [G_{00}(t)]} \right\} \frac{\partial G_{00}(t)}{\partial a_i} = 0$$

$$i = 1, 2, \cdots m_{a_i}$$

Because these equations are nonlinear they must be solved by an iterative procedure. The expressions for the second derivatives of the log likelihood function with respect to the Fourier coefficients a_i are

$$\frac{\partial^2 \log L_{00}}{\partial a_i \partial a_j} = -\sum_{t=1}^{365} \frac{N_D(t-1) \exp (G_{00}(t))}{[1 + \exp (G_{00}(t))]^2} \frac{\partial G_{00}(t)}{\partial a_i} \frac{\partial G_{00}(t)}{\partial a_j}$$

Note that $\partial G_{00}(t)/\partial a_i = \phi_i(t)$.

The Newton-Raphson procedure has proven to be effective in solving the simultaneous equations. Starting values for the coefficients are obtained by least squares fitting of Fourier series to logits calculated from estimates of p_{00} for 26 periods of 14 days each (15 days in the last period). We have used five harmonics (11 parameters) to describe $G_{00}(t)$. Missing data on either day t or $t - 1$ were ignored in determining $N_D(t - 1)$ and $N_{DD}(t)$.

Acknowledgments. We thank Richard Katz for helpful suggestion and Shams Vazirinejad for his assistance in programing.

REFERENCES

Akaike, H., A new look at the statistical model identification, *IEEE Trans. Autom. Control, 19*, 716–723, 1974.

Andrade, E. R., and W. D. Sellers, El Nino and its effect on precipitation in Arizona and western New Mexico, *J. Clim., 8*, 403–410, 1988.

Bryson, R. A., and F. K. Hare, The climates of North America, in *Climates of North America, World Survey of Climatology*, vol. 11, edited by R. A. Bryson and F. K. Hare, pp. 1–47, Elsevier Science, New York, 1974.

Buishand, T. A., Stochastic modeling of daily rainfall sequences, *Meded. Landbouwhogesch. Wageningen, 77-3*, 211 pp., 1977.

Caviedes, C. N., El Nino 1972: Its climatic, ecological and human implications, *Geogr. Rev., 65*, 493–509, 1975.

Caviedes, C. N., El Nino 1982–83, *Geogr. Rev., 74*, 268–290, 1984.

Cayan, D. R., and D. H. Peterson, The influence of North Pacific atmospheric circulation on streamflow in the West, in *Aspects of Climate Variability in the Pacific and Western Americas*, edited by D. H. Peterson, *Geophys. Monogr. Ser.*, vol. 55, 325–398, AGU, Washington, D. C., 1989.

Chu, P.-S., and R. W. Katz, Modeling and forecasting the Southern Oscillation: A time-domain approach, *Mon. Weather Rev., 113*, 1876–1888, 1985.

Currie, R. G., and D. P. O'Brien, Deterministic signals in precipitation in the northwestern United States, *Water Resour. Res., 26*, 1649–1656, 1990.

Enfield, D. B., El Nino, Past and Present, *Rev. Geophys., 21*, 159–187, 1989.

Horel, J. D., and J. M. Wallace, Planetary-scale atmospheric phenomena associated with the Southern Oscillation, *Month. Weather Rev., 109*, 813–829, 1981.

Kiladis, G. N., and H. F. Diaz, Global climate anomolies associated with extremes in the Southern Oscillation, *J. Clim. 2*, 1069–1090, 1989.

Lough, J. M., and H. C. Fritts, The southern oscillation and tree rings: 1600–1961, *J. Clim. Appl. Meteorol., 24*, 952–966, 1985.

Rasmussen, E. M., and J. M. Wallace, Meteorological aspects of the El Nino/Southern Oscillation, *Science, 222*, 1195–1202, 1983.

Redmond, K. T., and R. W. Koch, Surface climate and streamflow variability in the western United States and their relationship to large-scale circulation indices, *Water Resour. Res., 27*, 2381–2399, 1991.

Ropelewski, C. F., and M. S. Halpert, North American precipitation and temperature patterns associated with the El Nino/Southern Oscillation, *Mon. Weather Rev., 114*, 2352–2362, 1986.

Ropelewski, C. F., and M. S. Halpert, Global and regional scale precipitation patterns associated with the El Nino/Southern Oscillation, *Mon. Weather Rev., 115*, 1606–1626, 1987.

Ropelewski, C. F., and M. S. Halpert, Precipitation patterns associated with the high index phase of the Southern Oscillation, *J. Clim., 2*, 268–284, 1989.

Ropelewski, C. F., and M. S. Halpert, Uncovering North American temperature and precipitation patterns associated with the Southern Oscillation, Proc. Sixth Annual Pacific Climate (PACLIM) Workshop, *Tech. Rep. 23*, pp. 47–48, Interagency Ecol. Stud. Prog., Calif. Dept. of Water Resour., Sacramento, Calif., 1990.

Schonher, T., and S. E. Nicholson, The relationship between California rainfall and ENSO events, *J. Clim., 2*, 1258–1269, 1989.

Stern, R. D., and R. Coe, A model fitting analysis of daily rainfall data, *J. R. Stat. Soc., Ser. A, 147*, 1–34, 1984.

Swetnam, T. W., and J. L. Betancourt, Fire-Southern Oscillation relations in the southwestern United States, *Science, 249*, 1017–1020, 1990.

Webb, R. H., and J. L. Betancourt, Climatic effects on flood frequency: An example from southern Arizona, Proc. Sixth Annual Pacific Climate (PACLIM) Workshop, *Tech. Rep. 23*, pp. 62–66, Interagency Ecol. Stud. Progr. Calif. Dept. of Water Resour., Sacramento, Calif., 1990.

Wilks, D. S., Conditioning stochastic daily precipitation models on total monthly precipitation, *Water Resour. Res., 25*, 1429–1439, 1989.

Woolhiser, D. A., Modelling daily precipitation—Progress and problems, in *Statistics in the Environmental and Earth Sciences*, edited by A. Walden and P. Guttorp, pp. 71–89, Edward Arnold, London, 1992.

Woolhiser, D. A., and G. G. S. Pegram, Maximum likelihood estimation of Fourier coefficients to describe seasonal variation of parameters in stochastic daily precipitation models, *J. Appl. Meteorol., 18*, 34–42, 1979.

Woolhiser, D. A., and J. Roldan, Seasonal and regional variability of parameters for stochastic daily precipitation models: South Dakota, U.S.A., *Water Resour. Res., 22*, 965–978, 1986.

Woolhiser, D. A., C. L. Hanson, and C. W. Richardson, Microcomputer program for daily weather simulation, U.S. Dept. of Agric., Agric. Res. Serv., *ARS-75*, 49 pp., 1988.

Yarnal, B., and H. F. Diaz, Relationships between extremes of the Southern Oscillation and the winter climate of the Anglo-American Pacific coast, *J. Climatol., 6*, 197–219, 1986.

Zucchini, W., and P. T. Adamson, The occurrence and severity of droughts in South Africa, *WRC Rep. 91/1/84*, 198 pp., Dept. of Civ. Eng., Univ. of Stellenbosch and Dept. of Water Affairs, Pretoria, South Africa, 1984.

T. O. Keefer and D. A. Woolhiser, Agricultural Research Service, U.S. Department of Agriculture, 2000 East Allen Road, Tucson, AZ 85719.

K. T. Redmond, Western Regional Climate Center, P.O. Box 60220, Reno, NV 89506.

(Received April 30, 1992;
revised October 14, 1992;
accepted October 22, 1992.)